Journal of Power Sources 196 (2011) 25–38

Contents lists available at ScienceDirect

Journal of Power Sources

journal homepage: www.elsevier.com/locate/jpowsour

Review

Internal steam reforming in solid oxide fuel cells: Status and opportunities of kinetic studies and their impact on modelling

D. Mogensen[a], J.-D. Grunwaldt[b], P.V. Hendriksen[c], K. Dam-Johansen[a,*], J.U. Nielsen[d]

[a] Department of Chemical and Biochemical Engineering, Technical University of Denmark, Soltofts Plads Building 229, DK-2800 Kgs. Lyngby, Denmark
[b] Institute for Chemical Technology and Polymer Chemistry, Karlsruhe Institute of Technology (KIT), Engesserstrasse 20, D-76131 Karlsruhe, Germany
[c] Risoe National Laboratory for Sustainable Energy, Technical University of Denmark, Frederiksborgvej 399, DK-4000 Roskilde, Denmark
[d] Topsoe Fuel Cell, Nymollevej 66, DK-2800 Lyngby, Denmark

ARTICLE INFO

Article history:
Received 6 May 2010
Received in revised form 14 June 2010
Accepted 24 June 2010
Available online 1 July 2010

Keywords:
Internal steam reforming
Kinetics
Solid oxide fuel cells
Modeling
Ni-YSZ

ABSTRACT

Solid oxide fuel cells (SOFC) systems with internal steam reforming have the potential to become an economically competitive technology for cogeneration power plants, exploiting its significantly higher electrical efficiency compared to existing technologies. Optimal design and operation of such a system require SOFC models that include accurate description of the steam reforming rate. The objective of this article is to review the reported kinetic expressions for the steam reforming reaction. Extensive work has been performed on traditional catalysts for steam reforming. Because of differences in operating conditions, catalyst support material and structure it is critical to transfer this knowledge directly to internal reforming in SOFCs, which is discussed in further detail in this article. There are big differences in the reported kinetic expression for steam reforming over both industrial Ni catalysts and SOFC anode materials. Surprisingly, there is a good agreement between measured rates pr. geometric anode area at high operating temperatures, even for very different anodes. Detailed experimental data on the intrinsic steam reforming kinetics of Ni-YSZ are necessary for micro structure SOFC modeling, such expression are however lacking, but it may be viable to use measurements on industrial steam reforming catalysts instead. Nevertheless there is a further need for experimental studies on determining the exact steam reforming kinetics for SOFC anodes.

Contents

* Corresponding author. Tel.: +45 4525 2845; fax: +45 4588 2258.
E-mail address: KDJ@kt.dtu.dk (K. Dam-Johansen).

0378-7753/$ – see front matter © 2010 Elsevier B.V. All rights reserved.
doi:10.1016/j.jpowsour.2010.06.091

1. Introduction

Solid oxide fuel cells (SOFC) systems have a strong potential to become economically competitive with existing technologies for power generation, such as gas turbines in co-generation plants [1–3]. The striking advantage of fuel cells is that they directly convert fuel electrochemically to electricity and thus the efficiency is not limited by the Carnot cycle. In addition, high efficiency can be achieved in small units, applicable for power production for refrigerated trucks, mobile homes and other small scale applications [4]. Small power generation units also allow alternative fuel sources such as gasified biomass or agricultural biogas, to be harnessed to a greater extent, without expensive transportation [5–7].

Among the different types of fuel cells, SOFCs have attracted strong attention [8–14] due to the higher outlet temperature (ease of waste heat utilization), its fuel flexibility, and its resistance to some of the poisons that affect other fuel cells [4]. The most straightforward fuel in a fuel cell is hydrogen at present mainly produced from hydrocarbons. For low temperature fuel cell systems this hydrocarbon to hydrogen conversion is typically achieved by external steam reforming. In contrast, for SOFC's, internal steam reforming can also be applied, because the Ni containing SOFC anode support can act as a steam reforming catalyst and the operating temperature is suitable for methane conversion [15–17].

One of the advantages of internal steam reforming is that part of the heat generated in the cell by electrochemical reactions, and ohmic heating is directly used for the endothermic reforming reaction [3,18,19]. In consequence, less heat needs to be supplied for the pre-reformer and less cooling of the stack is needed. Both aspect decrease the operating costs of the system. Furthermore, the equipment costs are lower since a smaller pre-reformer is needed and finally more even temperature distributions in the SOFC, than with pure hydrogen can potentially be achieved, if proper control of the catalytic activity is achieved.

With the current SOFC technology, the internal steam reforming is much faster than the electrochemical reactions, which means that the temperature gradients are actually larger than for SOFC's running on pure hydrogen. By gradually removing heat and producing hydrogen through the cell, the temperature and concentration gradients can be decreased which could significantly improve its performance [20]. This requires, however, detailed knowledge of the kinetics of the steam reforming reaction in order to tune the conditions and the anode structure or composition.

The kinetics of the steam reforming reaction of nickel-based catalysts have been studied widely in literature, especially in catalytic reactors, because of the industrial importance of this process [21]. However, the studies have often been performed at conditions or on materials that are far from those of SOFC anodes. Only a few suitable kinetic data sets on real SOFC anode materials are available in literature.

The aim of this article is to give a present status on the available information on the internal steam reforming reaction over fuel cell anode catalysts. Focus is first laid on the material aspect followed in the second part by how the steam reforming activity can be tuned and which conditions are preferred for internal steam reforming over Ni-based anodes. The key part of the review focuses on a comparison of steam reforming kinetics on catalytic materials and in SOFCs. Finally, its impact on the modeling of solid oxide fuel cells is briefly discussed.

2. The structure of an SOFC

An SOFC is a continuously fed electrochemical cell, where the electrodes and electrolyte are ceramic materials. The major electrochemical reaction which takes place in an SOFC is the oxidation of fuel. A large variety of materials are used in SOFCs and novel materials are presented regularly [22–34]. Typical SOFCs use anode supported cells with [4,22–27]:

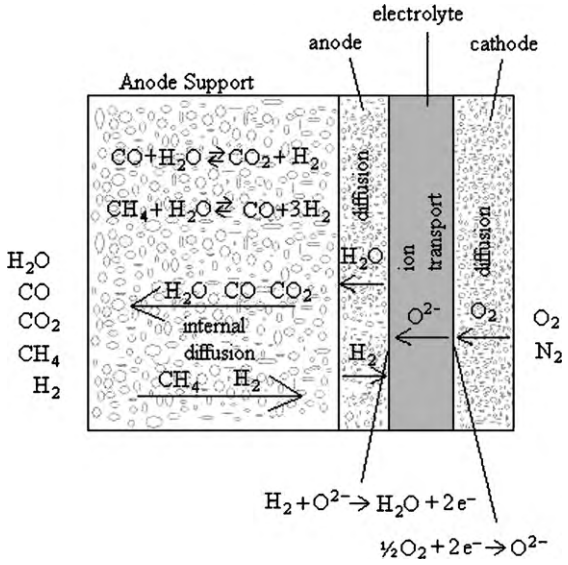

Fig. 1. Illustration of the structure and major processes of an anode supported SOFC.

- yttria stabilized zirconia (YSZ) electrolyte ($\tau_{el} \approx 10\mu m$).
- Ni-YSZ anode ($\tau_{an} \approx 10\mu m$) and support ($\tau_{sup} = 300 - 1000\mu m$).
- Strontium doped lanthanum manganate (LSM) cathode ($\tau_{cat} \approx 50\mu m$).

These thicknesses (τ_{el}, τ_{an}, τ_{sup}, τ_{cat}) are used as estimations later in this article. A cell is illustrated schematically in Fig. 1. Typical structural parameters for a Ni-YSZ SOFC anode support are: porosity ≈ 40–50%, Ni content ≈ 40 vol.% , $d_{p,Ni} \approx$ 1 μm [4,22–27]. The anode support can be manufactured by first tape casting a slurry of NiO and YSZ powders. The active anode, electrolyte and cathode are then sprayed or screenprinted on the anode support. The active anode normally has a composition similar to that of the support, but is denser. Finally, the NiO in the anode and anode support is reduced, which significantly increases the porosity [23,26,27,35]. Note, that the nickel particle size is much larger than in traditional steam reforming catalysts and the amount of nickel is significantly higher in order to ensure a high conductivity.

It is convenient to use Ni-YSZ as the structural backbone of the cell because it has desirable mechanical properties, low ohmic resistance and it allows preparation by cofiring of the entire cell, which decreases production costs [36].

3. Steam reforming catalyst

Steam reforming has been used for hydrogen production since 1930 and the process as well as the kinetics have been examined in numerous studies [21,37–43]. The most commonly used catalyst in this process is nickel on a support of α-Al_2O_3, MgO or $(Mg,Al)_3O_4$ spinel. The nickel loading is around 25% w/w, with nickel particles that are preferably smaller than 10 nm.

$$CH_4 + H_2O \leftrightarrows CO + 3H_2 \quad (1)$$

$$CO + H_2O \leftrightarrows CO_2 + H_2 \quad (2)$$

The steam reforming reaction (reac. 1) is highly endothermic (ΔH^o_{298} = 206 kJ mol^{-1}) whereas the water gas shift reaction (reac. 2) is slightly exothermic (ΔH^o_{298} = -41 kJ mol^{-1}), which means that energy must be supplied for the total reaction to proceed. A number of different existing reactor designs [42,44–46] allow for such

large energy supply. In the traditional industrial process the reaction takes place over catalyst particles in large number of vertical tubes. Heat is supplied by placing the tubes in a furnace, which is heated by combustion of natural gas [21,42]. The operating conditions of a typical industrial steam reforming process are 700–1000 °C with a pressure around 30 bar and a steam-to-carbon ratio (S/C) of 2.5–4 [39,47]. Often more than one reactor will be used in series, with different conditions. The first reactor is designed for high reaction rate and the subsequent reactors to increase output by shifting the equilibrium.

The catalyst in an SOFC is different from the commercial catalyst, even though nickel is also the main catalytic component. As described in Section 2, Ni is mixed with YSZ. Both the Ni content and particle size are significantly higher than in industrial steam reforming catalysts, to ensure a high electrical conductivity. Furthermore, the geometry is also different (thin plate). Operating conditions are: T = 600–1000 °C, S/C ≈ 1.5 and P = 1–15 bar [4]. High pressure is theoretically advantageous since it increases the cell voltage and improves electrode kinetics, but is non-trivial to realize in practice due to the brittle character of the cells and sealing used, which do not tolerate large pressure differences. The energy for steam reforming is supplied by the waste heat from the electrochemical reactions and ohmic heating. The continuous consumption of hydrogen in a SOFC and the requirement of high fuel consumption lead to complete conversion of methane.

It would be highly advantageous if the extensive knowledge gained in the industrial steam reforming process could be transferred to internal steam reforming in SOFCs. Despite nickel is the catalyst in both processes, the above descriptions show that the support material, catalyst structure and pressure are not similar. This means that knowledge from the industrial steam reforming process does not necessarily apply directly to internal reforming in SOFCs.

One of the major issues for internal steam reforming at the temperatures used in SOFCs today is that the reforming reaction is much faster than the electrochemical reactions. This is mainly due to the high nickel content, which is required for electric conductivity, but also offers a high number of catalytic sites. Steam reforming consumes energy and the electrochemical reactions produce energy and since the steam reforming is fastest, the result is cooling at the fuel inlet and heating at the fuel outlet. This introduces large temperature gradients, resulting in thermal stress and reduced efficiency [20]. The result is that in contrast to what is normally desired when investigating catalytic reactions, the goal for optimizing internal steam reforming is to lower the reaction rate of steam reforming, while maintaining high electric conductivity and high reactivity of the electrochemical reactions. The techniques used in industrial steam reforming for altering the reaction rate are also relevant for changing the reaction rate in SOFC. However, the goals are opposite i.e. lowering the reaction rate. The major challenge for industrial steam reforming is to avoid a reduction in activity by minimizing sintering, sulfur poisoning and carbon formation [38]. This is also relevant for internal steam reforming in SOFCs to achieve long-term performance.

3.1. Carbon poisoning

The deposition of elemental carbon on the catalyst is a major issue for both industrial steam reforming and SOFCs with internal reforming. The carbon may be formed by the methane cracking reactions shown below, and similar for higher hydrocarbons. It is especially important to be aware of carbon poisoning when using Ni-YSZ anodes, since these are vulnerable to carbon deposition [48].

$$CH_4 \rightarrow C + 2H_2 \quad (3)$$

$$2CO \rightarrow C + CO_2 \quad (4)$$

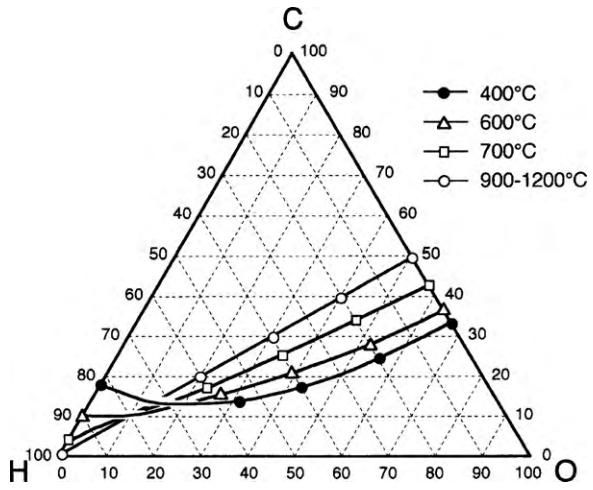

Fig. 2. Carbon deposition region in a C–H–O phase diagram at 1 atm [51], reproduced with permission from Elsevier.

Three different types of carbon depositions have been reported for industrial steam reforming catalysts: pyrolytic carbon, encapsulating carbon (gum) and whisker carbon. Pyrolytic and gum carbon reduce the catalyst activity and block the pores while whisker carbon destroys the structure of the catalyst [38,40,49,50]. Especially the destructive effect of whisker carbon must be avoided, both in SOFCs and industrial reforming.

The theoretical carbon deposition region has been determined by thermodynamic equilibrium calculations by several authors [51–54], and is shown as the area above the equilibrium lines in the phase diagram depicted in Fig. 2. The curvature of the low temperature lines at high hydrogen content illustrates that CH_4 becomes stable under these conditions. Moreover the carbon deposition region shrinks with increasing temperature, but the rate of carbon formation is reported to increase with temperature [48,49,55]. Fig. 2 shows that carbon deposition should not occur for O/C > 1 at 900–1200 °C (corresponding to S/C > 1 at the inlet) and at lower temperatures higher O/C ratios are needed. In a model study by Hsiao et al. [56] it was reported that the most critical point for carbon deposition occurs about one quarter down the fuel channel. This is caused by two partly compensating effects: oxygen is moved to the anode side in the electrochemical reactions, which shifts the gas composition away from the carbon deposition region, and the cooling of the cell caused by the endothermal steam reforming reduces the temperature, which increases the carbon deposition region. No carbon deposition was observed for S/C ratios higher than 1.5–1.6 on Ni-YSZ in an SOFC [52,57], but higher S/C ratios are needed to avoid carbon deposition from higher hydrocarbons [48,51,58,59]. The lower the fuel utilisation the higher S/C ratio is needed to avoid carbon deposition [52].

In the industrial steam reforming process carbon deposition is normally avoided by using a relatively high S/C ratio. However, in SOFCs the S/C ratio should be kept as low as possible since water is a product in the electrochemical reactions, and as such a higher steam content in the fuel will decrease the reversible cell voltage (U_{rev}), as seen from the Nernst equation below.

$$U_{rev} = -\frac{\Delta G}{2F_A} + \frac{R_g T}{2F_A} ln\left(\frac{P_{O_2}^{0.5} P_{H_2}}{P_{H_2O}}\right)$$

A lowering of the S/C ratio in industrial steam reforming will result in a reduction in equipment cost, so methods for avoiding carbon depositions at low S/C have long been searched for [47]. In situ microscopy studies reported by Sehested [38,60] show that step sites on the Ni catalyst particles are the most active nucleation

sites for both carbon formation and steam reforming. This is backed up by density functional theory calculations [61,62] and is in line with the observation that potassium, sulfur and gold reduce carbon formation by blocking these step sites [13,14,47,63–65]. Blocking the step sites also significantly reduces the steam reforming rate, which makes this method one of the most promising ones for reducing carbon deposition in SOFCs with internal steam reforming. New approaches to lowering carbon deposition by adding different promoters (Sn, Mo, Li, n-butanethiol, Mg, Ca, Sr, Ce, Ru, Rh, Pd, Pt) to the Ni-YSZ anode, are regularly reported in literature [54,66–69].

3.2. Effect of current

It has been shown that a sufficiently high cell current prevents carbon deposition, even for a cell fueled by methane with 3 % H_2O (S/C = 0.03) [70–73]. Lin et al. [70] suggested that deposited carbon is reoxidised by the oxygen ions passing through the electrolyte, but another possible explanation is that backflow of steam produced in the electrochemical reactions increases the local S/C ratio to values were elemental carbon is not formed. The necessary minimum cell current density is greatly dependent on temperature. At 700 ° C a current of approximately 0.1 A cm^{-2} is needed while at 800 °C, 1.8 A cm^{-2} is needed. The minimum cell current density is, most likely, highly dependent on the total flow, and this should also be investigated (The flow used by Lin et al. [70] was 30 sccm on a anode area of 2.8 cm^2 with a thickness og 0.7–1 mm). Such a high current density will with present day state of the art cells mean that one has to operate at very low voltage unlikely to be optimal from an overall cost point of view. It has been shown that it is possible to decrease the necessary current with up to a factor 3 by applying an inert barrier layer on the anode support. This is most likely caused by increased mass transport limitations, which in turn should also decrease the rate of the electrochemical reactions. A further investigation of the effect of such an inert layer would be very interesting. There are, however some fundamental difficulties, with using pure methane fuel and relying on current to prevent carbon deposition. Natural gas contains higher hydrocarbons, which have a much higher tendency for carbon deposition, meaning that some degree of external purification is needed. Also, it is highly problematic if a commercial cell is not tolerant towards sudden drops in current. The possibility of direct electrochemical oxidation of methane in SOFC has been shown [74], however with high polarization resistance. Recently, some groups have reported fast direct electrochemical oxidation of methane [75–77], however, it has been debated [78] whether it is direct electrochemical oxidation of methane or rather oxidation via an indirect route, e.g. cracking of methane with subsequent oxidation of carbon or possibly via partial steam reforming followed by electrochemical oxidation of hydrogen and CO.

3.3. Finetuning of catalyst

In SOFC systems running on natural gas with internal steam reforming, some degree of pre-reforming is necessary to avoid carbon formation due to higher hydrocarbons and decrease the methane concentration to a level that result in acceptable temperature and concentration gradients in the SOFC stack [18,79]. There is, however, potential for significant improvement of the system efficiency by lowering the degree of pre-reforming and reducing the temperature and concentration gradients in the stack. A possible strategy, is to lower the reforming rate to the same level as the electrochemical reactions. In fact, the general tendency of today's SOFC research is to lower the operating temperature [80–82] and since the steam reforming reaction has a high activation energy (58–228 kJ mol^{-1}, see Table 5), the reaction rate decreases rapidly with temperature. The present lower temperature limit for efficient operation of an SOFC is around 650–700 ° C [25,82]. In order to illustrate the temperature dependency of internal steam reforming, order of magnitude calculations were made based on the steam reforming rate by Wei et al. [40] (E_A = 102 kJ mol^{-1}), which is later used as a reference expression. The calculations are made for a 1 cm^2 Ni-YSZ anode with thickness = 500 μm, Ni content = 50% (w/w), Ni particle size = 1 μm and porosity = 50%, Gas composition: 50/50 methane and water and no mass transport limitation for steam reforming. The resulting rate of hydrogen production from steam reforming is shown in Table 1. The efficiency factor in Table 1 is calculated from Eq. (5) and describes how big a fraction of the available catalyst material that is being fully used, i.e. an efficiency factor = 1 corresponds to full usage of the catalyst [42].

Table 1
Theoretical hydrogen production rate from steam reforming in 1 cm^2 of an SOFC anode, using the kinetic expression by Wei et al. [40], details see text.

T°C	$r_{H_2,prod}$ mol $s^{-1}cm^{-2}$	$i_{equivalent}$ A cm^{-2}	η
400	4.3E-07	0.08	0.99
500	4.8E-06	0.9	0.97
600	3.1E-05	5.9	0.84
700	1.3E-04	26	0.58
800	4.5E-04	86	0.34
900	1.2E-03	233	0.21

$$\eta = \frac{Tan\,h(\phi)}{\phi} \tag{5}$$

where ϕ is the Thiele modulus:

$$\phi = L\sqrt{\frac{k}{D}}$$

where L is the anode thickness, k is the rate constant (s^{-1}) and D is the diffusion coefficient (m^2s^{-1}). The diffusion coefficient of methane is assumed to be 10^{-5} m^{2s-1}. $i_{equivalent}$ is the theoretical current that corresponds to a consumption of hydrogen in the same rate as it is produced from the steam reforming reaction, calculated from:

$$i_{equivalent} = 2F_A r_{H_2,prod}$$

where F_A is the Faraday constant.

These calculations illustrates how the rate of the steam reforming reaction compares to the rate of electrochemical reactions. For optimal operation, without hydrogen i the inlet gas, $i_{equivalent}$ should probably be a little higher than the operating current. This means that at temperatures 600–700 ° C the rate of steam reforming rate is in a range where it should be possible to reduce it to the desired level by finetuning the catalyst. It should be noted however, that during the calculation of $i_{equivalent}$ it was assumed that the steam reforming rate was not limited by diffusion. The η values show that this assumption is only valid at low temperatures, meaning that at high temperatures the actual rate will be lower than the one calculated here.

Another theoretical possibility for decreasing the steam reforming rate, by changing the conditions, is to have a low S/C ratio in the fuel inlet, so that the conversion of methane will be controlled by equilibrium and thereby the amount of water produced in the electrochemical reaction. However, this will result in significant carbon deposition in the cell as described in Section 3.1.

Up to now, alternative materials has been hampered by low electronic conduction. For example, Georges et al. [15] has presented a strontium doped lanthanum chromite impregnated with ruthenium catalyst (LSCRu), which operates at S/C ratios down to 0.08 without carbon deposition. Unfortunately, this material has very poor anode properties, so this study can only be considered a proof of concept, not a solution.

Rostrup-Nielsen et al. [14] conclude that the catalytic steam reforming of methane does not take place at the same catalytic sites as the electrochemical conversion of hydrogen. It might therefore be possible to further decrease the steam reforming reaction rate by selectively blocking the catalytic sites without significantly lowering the cell performance. Several possible methods for doing this originating from the research on preventing poisoning of industrial reforming catalysts are described in the following sections.

3.3.1. Particle size

The size of nickel particles in the anode support will influence the steam reforming rate because larger particles give a smaller surface area for the same nickel content and thereby less active sites for catalysis. If the particle size in the active anode is also increased it can however result in a smaller triple phase boundary between anode, electrolyte and gas, which is the active area for the anode reaction [83–85]. It was shown by Simwonis et al. [86] that the nickel particle size also influences the electrical conductivity of the anode and that the particle size increases during operation by agglomeration, which is in fact one of the major anode degradation mechanisms [38,86,87]. This means that an increase in Ni particle size in order to reduce the steam reforming reaction rate may result in a reduction in cell performance. Note however that nickel particle size in SOFC anodes is in general much larger than in industrial steam reforming catalysts.

3.3.2. Sulfur

Several studies on the effects of sulfur on the fuel cell performance of NI-YSZ anodes operating in hydrogen have been reported in literature [64,88–94]. Exposing an operating cell to ppm levels of sulfur in the anode stream results in an immediate voltage drop (few minutes up to few hours) followed by a slower decay of the voltage occurring over the following hundred hours [89]. In hydrogen under the studied current loads (less than 1A cm^{-2}) the effect of the sulfur poisoning seems fully reversible—the cell voltage returns slowly (over 10 to few hundreds hours) to its original value after removal of the sulfur [89,90]. The effects of sulfur on Ni catalysts and SOFC anodes has recently been reviewed by Hansen and Nielsen [95]. The poisoning is due to adsorption of sulfur on sites active in the electrochemical reaction [95]. Both the temperature dependence and the dependence on sulfur concentration of the experimentally observed voltage losses can be accounted for assuming that the loss scales in a linear manner with the sulfur coverage on the Ni, the temperature and H_2S partial pressure dependence of which is known assuming that the adsorption follows a Temkin-like isotherm [95].

Only few reports are available on the effects of sulfur on the electrochemical processes considering operation in CO/H2/H2O/CO2; Noponen [96] reports only a small adverse effect of sulfur (at 800 °C, $i = 0.5\ A\ cm^{-2}$) and Silversand [14,97] reports in a short-term test that there are no irreversible degradation of the electrochemical performance of up to 50 ppm H2S at 700–800 °C.

Interestingly, it has been reported that the effects of sulfur on the SOFC Ni-cermet anode performance is strongly affected by the ceramic part of the anode: Sasaki finds that a Ni/SzSZ is more robust toward sulfur poisoning than a similar NI-YSZ anode and that the tolerance can be further increased by various oxide additions (e.g. Ce-oxide, Y-oxide, La-oxide) [88].

It has clearly been demonstrated [95,97,98], that sulfur adsorption in the anode has a much stronger impact on the steam reforming rate than it does on the electrochemical processes and hence, slowing down of the reforming rate by controlled sulfur poisoning is an interesting technological possibility [99,100]. However, more studies are needed to map out the span of operation conditions and sulfur levels that will not lead to non-recoverable loss of the electrochemical performance of the cell.

3.3.3. Alkali and earth alkali metals

Rostrup-Nielsen and Christiansen [63] reported that the rate of catalytic steam reforming over 7–9% Ni on Mg/Al-spinel is significantly reduced by addition of alkali metals. An explanation of this is suggested from DFT calculations, which show that blocking of step sites will significantly reduce catalyst activity [61,62] and alkali metals absorb to step sites. The reduction in activity was shown to be a factor 2–5 depending on the alkali metal. Alkali poisoning is thus a promising method for finetuning of catalytic activity in SOFCs.

Kikuchi and coworkers [54,58] investigated the change in carbon deposition and steam reforming rate when adding CaO, MgO, SrO and CeO_2 to Ni-YSZ anodes in the temperature range 600–800 °C. CaO and SrO decreased carbon deposition with 30–50% while Mg increased it with up to 20%, low amounts of CeO_2 (0.2%, w/w) decreased the carbon deposition (≈50%) while high amounts (2%, w/w) increased carbon deposition (≈25%). In most cases the addition of the alkaline earth metals to Ni-YSZ resulted in a slight increase in steam reforming rate, with the following 3 exceptions: A high amount of SrO almost removed the catalytic effect of nickel (whereas low amounts increased activity), small addition of MgO reduced reforming rate by about 40% and high amounts of CeO_2 decreased reforming rate with up to 75%. From this it can be concluded that MgO and CeO_2 in the right amounts could possibly be used for reducing steam reforming rate in SOFC's, but it has to be considered that both of these increase carbon deposition. It should be noted that the Ni-YSZ in these investigations contained 75–80% Ni (w/w), which is very high for an SOFC anode.

3.3.4. Modified Ni-YSZ anodes and Ni substitution

The suggestions for finetuning the anode catalyst in the previous sections by larger particles and poisoning by sulfur or alkali metals have the disadvantage that the electrochemical reactions are also influenced. Another method for lowering the steam reforming rate is modification of Ni-YSZ or using entirely different anode materials. Note, however, that other requirements also have to be considered, such as low electric resistance, high porosity and a thermal expansion coefficient similar to the active anode, electrolyte and cathode.

A promising work on modifying the anode was presented by Boder and Dittmeyer [79], who reported that replacing some of the nickel in the anode with copper reduces the steam reforming rate with a factor 4-20 without significant reduction in electrochemical performance. Further investigations into this direction could be rewarding.

An SOFC with an anode catalyst layer consisting of Ir impregnated Ceria on top an active anode of Ni-YSZ is reported by Klein et al. [12] to operate on pure methane for almost 30 h without showing signs of degradation, i.e. carbon deposition. The power production during this experiment was only about 55 mW m^{-2}, so the performance of this type of cell has to be greatly improved in order to be relevant. Ru and Pt additives have also been reported to prevent carbon deposition on Ni-YSZ for internal steam reforming with S/C as low as 0.1 [54,101].

Gorte and coworkers [102–104] report the use of Cu–CeO_2–YSZ. It is applicable for higher hydrocarbons but has lower affinity toward hydrogen oxidation in the triple phase boundary. A fuel cell with Ni-YSZ as the active anode and Co–Ni–SDC as support material and steam reforming catalyst has been tested with pure methane as the fuel with no observed carbon deposition. The cell performances were however relatively poor, with a maximum power density of 0.35 W cm^{-2}, which decreased significantly with time [105]. Finally, a Ni-YSZ anode coated with a layer of catalytically inert YSZ was proposed to reduce the steam reforming rate due to mass transport, but there is disagreement about the effect on the electrical efficiency [70–72,106–108]. On a side note, these find-

Table 2
Langmuir–Hinshelwood steam reforming kinetics reported for Ni catalysts. (The constants in the table are: k overall rate constants, K equilibrium constants, the subscript ad is adsorption of the denoted species and a roman numeral in the subscripts refers to reactions 1–11. $(1 - Q_i/K_i)$ describes the approach to equilibrium of reaction i where Q is defined in Eq. (6), and at equilibrium $Q = K$.)

	RDS	Expression	Support	T [°C]	P_{tot} [bar]	S/C	Ref.
A)	Classical	$r = \frac{kP_{CH_4}P_{H_2O}}{P_{H_2}^{2.5}Z^2}\left(1-\frac{Q}{K}\right)$ [a]	$MgAl_2O_4$	500–575	3–15	3–5	[39]
	(Eq. 1)	$+\frac{k'P_{CH_4}P_{H_2O}^2}{P_{H_2}^{3.5}Z^2}\left(1-\frac{Q'}{K'}\right)$	spinel				
B)	Classical	$r = k\frac{K_{ad,CH_4}K_{ad,H_2O}P_{CH_4}P_{H_2O}}{\left(1+K_{ad,CH_4}P_{CH_4}+K_{ad,H_2O}P_{H_2O}\right)^2}$	YSZ-CeO	700–1000	-	2–7	[111]
C)	Classical	$r = k\frac{K_{ad,CH_4}K_{ad,H_2O}P_{CH_4}P_{H_2O}}{\left(1+K_{ad,CH_4}P_{CH_4}+K_{ad,H_2O}P_{H_2O}+K_{ad,CO}P_{CO}\right)^2}$	YSZ	700–1000	-	3–7	[110]
D)	$CH_4 + * \leftrightarrows CH_2^* + H_2$	$r = \frac{k_1P_{CH_4}}{1+k_2\frac{P_{H_2O}}{P_{H_2}}+k_3P_{CO}}$	Ni foil	700–900	1	1.6–25	[37]
E)	1, 7	$r = k_{ad,CH_4}P_{CH_4}\left(1-\frac{k_{ad,CH_4}}{K_{vii}K_{ad,H_2O}}\frac{P_{H_2}P_{CH_4}}{P_{H_2O}}\right)$	YSZ	800–900	1	0–2	[73]
F)	1,7	$r = k\frac{P_{CH_4}}{\left(1+K_{ad,H_2}P_{H_2}^{1/2}+K_{ad,H_2O}\frac{P_{H_2O}}{P_{H_2}}\right)^2}$	ZrO_2	700–1000	1	1–3	[113]

[a] Where $Z = 1 + K_{ad,CO}P_{CO} + K_{ad,H_2}P_{H_2} + K_{ad,CH_4}P_{CH_4} + \frac{K_{ad,H_2O}P_{H_2O}}{P_{H_2}}$ and $'$ denotes overall reaction: $CH_4 + 2H_2O \leftrightarrows CO_2 + 4H_2$

ings suggest that it would be interesting to investigate a system with Ni-YSZ as the active anode, to ensure high electrochemical activity, and a copper containing Ni-YSZ anode support, to lower the steam reforming rate.

4. Steam reforming kinetics

The kinetic behaviour of the steam reforming reaction has been extensively studied over Ni supported model and industrial catalysts [21,37,39–41,43]. More recently, also the kinetics over Ni-YSZ anodes have been reported [9,79,109]. The reported kinetics seem to be significantly different, but this may be because the reaction conditions vary a lot in the different studies. Moreover, due to the high temperatures applied, mass and heat transport effects are difficult to control. A full kinetic analysis over a wide range of conditions has only been given in a few cases. The studies can be grouped in three according to which type of kinetic expression is used in the analysis of the experiments:

- General Langmuir–Hinshelwood kinetics.
- First order reaction with respect to methane.
- Power law expressions derived from data fitting.

First investigations on industrial and model catalyst systems shall be discussed in Sections 4.1–4.3 for the three types of kinetics. Subsequently a review of the available studies carried out on SOFC anodes is given in Section 4.4. An overview of the used kinetic expression and references can be found in Tables 2–4 for the model and industrial catalysts and in Tables 5 and 6 for the SOFC anode studies. When trying to compare kinetics reported for different SOFC anodes and between anodes and model systems, it should be noted that the microstructure of the Ni particles in Ni-YSZ may not be stable. Firstly, the Ni grain size distribution has been reported to have large fractions in two different sizes, the large Ni particles (0.3–2 μm) which are needed in SOFC anodes to ensure a high electrical conductivity, and small Ni particles (10–30 nm), which have a significant influence on the catalytic activity [9]. Secondly, sintering both increases particle size of the small particles, and removes some highly active reaction sites, for both small and large particles [9]. Thirdly, it has been shown that Ni particles are highly dynamic and can dramatically change structure during operation [60]. These effects are very difficult to describe accurately and this should be kept in mind when evaluating kinetic expressions.

4.1. Langmuir–Hinshelwood kinetics

The classical approach of Langmuir–Hinshelwood kinetics is derived from the reaction of surface species. Mainly two mech-

Table 3
First order steam reforming kinetics reported for Ni catalysts.

Expression	Support	T [°C]	P_{tot} [bar]	S/C	References
$r = kP_{CH_4}$	none	700–900	1	-	[121]
	ZrO_2-CeO	800–850	1	2–4	[122]
	Ceria	-	-	-	[50]
$r = kP_{CH_4}\left(1-\frac{Q_{sr}}{K_{sr}}\right)$	MgO	600–700	1–15	0–10	[40]
	YSZ	650–950	-	2	[79]
	ZrO_2	700–940	1.1–2.8	2.6–8	[109]

Table 4
Power law steam reforming kinetics reported for Ni catalysts.

Expression	Support	T [°C]	P_{tot} [bar]	S/C	References
$kP_{CH_4}^{1.19}$	CGO	800–950	1	0–3	[123]
$kP_{CH_4}^{0.85}P_{H_2O}^{-0.35}$	YSZ	850–900	1	1.53–2.5	[124]
$kP_{CH_4}P_{H_2O}^{-1.28}$	ZrO_2	800–1000	1	2–8	[65]
$kP_{CH_4}^{1.20}$	ZrO_2	900–1000	1	1.5–2.5	[125]
$kP_{CH_4}^{1.3}P_{H_2O}^{-1.2}$	YSZ	-	-	-	[126]

anistic schemes have been considered. The classical mechanism, presented first by Xu and Froment [39], postulates that the reaction of adsorbed carbon and oxygen species is the rate determining step (RDS) as shown below.

- $CHO^{*+*} \leftrightarrows CO^{*} + H^{*}$
- $CO^{*} + O^{*} \leftrightarrows CO_2^{*}$
- $CHO^{*} + O^{*} \leftrightarrows CO_2^{*} + H^{*}$

From this they conclude that the reaction rate is dependent on partial pressure of methane, water and hydrogen as shown in entry A in Table 2. Similar kinetics (without the strong hydrogen dependence) was used for Ni-YSZ, by Peters et al. [110] and Nakagawa et al. [111] as given in entry B and C in Table 2. The positive influence of water predicted by entries A, B and C is, however, rarely observed in literature. The value Q in expressions A, B and C is defined by:

$$Q = \frac{\prod P_{products}}{\prod P_{reactants}} \quad (6)$$

The term connected with Q, which appear in some of the kinetic expressions accounts for the backwards reaction close to equilibrium. In more recent work it has been shown that dissociative adsorption of methane is the rate limiting step (step 1). This leads to the following model for the elementary reactions, which nowadays is often used to derive kinetic expressions for steam reforming [42,112,40].

1. $CH_4 + 2^{*} \rightarrow CH_3^{*} + H^{*}$
2. $CH_3^{*} + {}^{*} \leftrightarrows CH_2^{*} + H^{*}$
3. $CH_2^{*} + {}^{*} \leftrightarrows CH^{*} + H^{*}$
4. $CH^{*+*} \leftrightarrows C^{*} + H^{*}$
5. $H_2O + 2^{*} \leftrightarrows HO^{*} + H^{*}$
6. $HO^{*+*} \leftrightarrows O^{*} + H^{*}$
7. $C^{*} + O^{*} \leftrightarrows CO^{*+*}$
8. $C^{*} + HO^{*} \leftrightarrows CHO^{*+*}$
9. $CHO^{*+*} \leftrightarrows CO^{*} + H^{*}$
10. $CO^{*} \leftrightarrows CO^{+*}$
11. $2H^{*} \leftrightarrows H_2 + 2^{*}$

It is generally agreed that Reaction 1 is an RDS, but there is great disagreement on whether or not reactions 5 and 7 should also be considered as RDS. The Langmuir–Hinshelwood expressions that have been reported for steam reforming over Ni-YSZ are presented in Table 2 along with some expressions for Ni on other support materials. Langmuir–Hinshelwood expressions are often presented with only a few rate and equilibrium constants, which are not connected to a specific elementary reaction, like in the last three expressions in Table 2. When observing such expressions it is important to remember that these constants are a combination of rate and equilibrium constants for several different elementary steps. This is especially relevant when the activation energy is reported without a derivation or indication of which elementary step(s) are rate determining [110,111].

There seems to be a consensus on a reaction order of 1 for methane. However, the expressions in entry E and F indicate another rate-limiting step than only the dissociative adsorption of methane. This is in line with the results of Aparicio et al. [41]. In addition, the effect of other adsorbates are considered in D and F as well as the reverse reaction in entry F. Expressions E and F are Langmuir-Hishelwood expressions that can be derived from the elementary reactions in Eqs. (1)–(11), D origins from an earlier, but similar set of elementary reactions.

A possible explanation for the many different expressions is given by density functional theory calculations, which show that reactions 1 and 7 are kinetically controlling, and that reaction 1 is rate controlling at high temperature while 7 (or another CO formation reaction) is rate controlling at low temperatures [114,115]. Hence the kinetic expression will change with operating conditions. Furthermore, it must be kept in mind that a large number of different plausible expressions can be derived from Langmuir–Hinshelwood kinetics with several constants in each expression. This means that an agreement to experimental data is not a definite proof for a mechanism.

4.2. First order kinetics with respect to methane

The Langmuir–Hinshelwood kinetics with dissociative adsorption of methane as the only rate determining step (Reaction 1) results in a first order expression that is only dependent on the methane partial pressure, under the assumption that the surface is not covered by other adsorbents. This assumption is valid at high temperatures and low pressure and since these conditions are normally used in experiments designed for investigating kinetic expression, this type of expression has received much attention. Several studies reporting first order kinetics are presented in Table 3.

A very extensive work on determining steam reforming kinetics at high temperatures has been performed by Wei and Iglesia, where steam reforming kinetics have been determined for a number of different metal-based catalysts, including Ni [40,116–120]. The experiments were conducted in packed catalyst beds. By changing the catalyst pellet size and the degree of dilution in the bed, mass transport effects could be excluded in these studies. The results were corrected for approach to equilibrium as shown in Eq. (7).

$$r_n = r_f \left(1 - \frac{Q_{sr}}{K_{sr}}\right) \quad (7)$$

where r_n is the net CH_4 conversion rate, r_f is the forward reaction rate, K is the equilibrium constant of the steam reforming reaction and Q is given by Eq. (6). The forward reaction rate was found to be first order in CH_4 and independent of the H_2O and CO_2 content, resulting in the simple expression in Eq. (8) for all the examined catalysts. The first order dependence in methane is in agreement with the majority of the reported steam reforming kinetics, but the independence of other gasses is less commonly reported.

$$r_f = kP_{CH_4} \quad (8)$$

Wei and Iglesia also examined the steam reforming and water gas shift reactions by isotopic tracing of some of the elementary steps, showing that they are in quasi-equilibrium. The results are summarized in Fig. 3, underlining that the rate determining step is activation of the first C–H bond (reaction 1), resulting in a first order expression for steam reforming with water gas shift and hydrogen formation/dissociation in quasi-equilibrium.

More recently, Hecht et al. [112] reported a combined model and experimental study of internal steam reforming over Ni-YSZ. They conclude that their findings on Ni-YSZ are consistent with the result of a first order expression with activation of the first C–H bond, found by Wei and Iglesia. However, an overall reaction rate for the steam reforming reaction is not explicitly presented. The model in this work is described in more detail in Section 6.

Achenbach and Riensche's [109] study of steam reforming kinetics over Ni on a zirconia support is focused on use for SOFCs and the determined kinetic expression for the initial rate is also first order in methane. The study takes into account the mass transport by using Newtons law for convective mass transfer (analogue to Fick's law), and uses an approach to equilibrium term like the one used by Wei and Iglesia, shown in Eqs. (7) and (6).

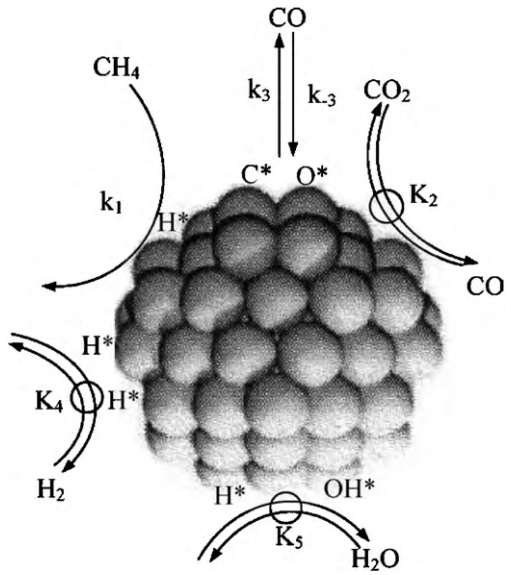

Fig. 3. Sequence of elementary steps for steam reforming and water gas shift reaction on Ni catalysts, as found by isotopic analysis. → irreversible step, ⇄ reversible step, (⇄), quasi-equilibrated steps, k_i is the rate constant and K_i is the equilibrium constant for reaction i [40], reproduced with permission from Elsevier.

4.3. Power law expressions

The kinetic expressions presented in Section 4.1 rely on several assumptions and simplifications (a single RDS, one dominating species on the surface, quasi equilibrium, etc.). To have a model independent description, many of the measured kinetics are instead given by power law expressions without tracing back to a mechanism of elementary steps. Kinetic measurements of the steam reforming reaction are normally fitted to the following power law expression.

$$-r_{CH_4} = kP_{CH_4}^{\alpha} P_{H_2O}^{\beta} P_{H_2}^{\gamma} P_{CO_2}^{\delta} P_{CO}^{\lambda} \quad (9)$$

γ, δ and λ are often found to be close to zero (see Table 4). The rate constant, k, as well as α and β vary between different studies. An overview of the reported power law expressions for steam reforming over Ni catalysts on either ceria or zirconia support is shown in Table 4. The reaction order with respect to methane is close to 1 for all expressions, in agreement with the expressions presented in Sections 4.1 and 4.2. There is, however, no agreement on the reaction order with respect to water. This may be due to the different conditions used in these studies. It is striking that many report the order to be negative.

Unfortunately, in many of the studies that present power law kinetics the experimental method does not follow the recommended practice for measuring catalytic reaction rates as described in "Concepts of Modern Catalysis and Kinetics" [42]. Some works do not comment on the possible effects of mass transport [124] and others have a high degree of conversion across the reactor (50–95%) giving strong temperature and concentration gradients along the reactor [65,125,123]. Temperature gradients imply that the actual temperature in the catalyst material will differ from the measured temperature and high concentration gradients mean that approach to equilibrium may influence the results. These uncontrolled effects are probably an additional cause for the disagreement on the reaction order with respect to water partial pressure. When using power law kinetics, it must be kept in mind that they are often used to describe measurements that are specific to the setup they are measured on, and in such cases they will probably not be representative for another system.

4.4. Kinetics over Ni-YSZ anode catalysts

Steam reforming kinetics for SOFCs have been investigated since the late 1980s but there is still no consensus on the kinetic expression [50,127]. In this section a comparison of the reported expressions is given as follows:

1. Reaction orders and experimental conditions.
   - Kinetic expressions (i.e. reaction orders) and activation energies are given in Table 5.
   - Experimental conditions of the compared expressions are summarized in Table 6.
2. Comparison of predicted rate under specific conditions normalized by:
   - Ni weight, Fig. 4.
   - Ni surface area, Fig. 5.
   - Geometric anode area, Fig. 6.

Besides the studies that are discussed here, additional experiments exist in the literature [8,79,110,113,126,131–133]. These studies were not included in this comparison because of insufficient information on experimental details to allow for appropriate calculations.

As can be seen in Table 5, there is a large spread in the reported activation energies (E_A), i.e., 58–229 kJ mol^{-1}, but the majority of the reported E_A lies just below 100 kJ mol^{-1}, which also fits well

Table 5
Steam reforming kinetics and activation energies reported for steam reforming over Ni-YSZ SOFC anode/anode-supports.

Expression	E_A [kJ mol^{-1}]	T [°C]	P_{tot} [bar]	S/C	References
$k_{ad,CH_4}P_{CH_4}\left(1-\frac{k_{ad,CH_4}}{K_5K_{ad,H_2O}}\frac{P_{H_2}P_{CH_4}}{P_{H_2O}}\right)$	228.8	800–900	1	0–2	LH1 [73]
kP_{CH_4}	113–124	650–800	-	3–15	SLH1 [9]
$kP_{CH_4}\left(1-\frac{Q}{K}\right)$	63.3	650–950	-	2	SLH2 [79]
$kP_{CH_4}\left(1-\frac{Q}{K}\right)$	82	700–940	1.1–2.8	2.6-8	SLH3 [109]
$kP_{CH_4}P_{H_2O}^{-1.25}$	74–98	800–1000	-	2–8	PL1 [65]
$kP_{CH_4}^{1.20}$	58	900–1000	-	1.5–2.5	PL2 [125]
$kP_{CH_4}^{0.85}P_{H_2O}^{-0.35}$	95	850–900	1	1.5–2.5	PL3 [124]
$kP_{CH_4}^{1.3}P_{H_2O}^{-1.2}$	191	-	-	-	[126]
$k_1\frac{K_{ad,CH_4}K_{ad,H_2O}P_{CH_4}P_{H_2O}}{\left(1+K_{ad,CH_4}P_{CH_4}+K_{ad,H_2O}P_{H_2O}+K_{ad,CO}P_{CO}\right)^2}$	-	700–1000	1	3–7	[110]
$k^+P_{CH_4}P_{H_2O}-k^-P_{CO}P_{H_2}^3$	-	700–950	1.5	3	[128,129]
$kP_{CH_4}P_{H_2O}\left(1-\frac{Q}{K}\right)$	205	600–700	-	2–3.5	[130]

Table 6
Ni-YSZ properties and measuring conditions for the compared expressions.

Expression/reference	Setup	Preparation	T [°C]	Thickness [mm]	Ni content [% w/w]	$A_{Ni,surf}$ [m^2 g_{anode}^{-1}]	dp_{Ni}[μm]	Porosity
LH1 [73]	cermet film	Precipitation	800–900	0.01	70	0.83	0.88 [a]	-
SLH1 [9]	PFR	Tape Casting	650–800	0.075–0.150 [b]	50	0.18	10–2000	-
SLH2 [79]	anode	Coat mix	650–950	0.04	65	1.2	0.4 [c]	-
SLH3 [109]	anode	- [c]	750–950	1.4	20	-	-	-
PL1 [65]	CSTR	4 different	800–1000	2.4–4.8 [b]	50–80	-	-	0.14–0.66
PL2 [125]	anode	Spray paint	900–1000	0.04	60 vol.%	-	-	-
PL3 [124]	anode	Screen print	850–900	0.05	-	-	-	-
Ref. [40]	PFR	-	600–700	0.25–0.45	7	1.8	0.0067	-

[a] Estimated value, assuming spherical Ni particles.
[b] Particle diameter of crushed anode.
[c] ZrO_2 support.

with the value of 102 kJ mol^{-1} reported by Wei and Iglesia [40] on an industrial steam reforming catalyst. There is, however, also a large spread in the activation energies reported for industrial steam reforming catalysts, for example the studies i Refs. [37,39,40,121] report values in the range 102–240 kJ mol^{-1}. In general the reported values seems to be higher than for Ni-YSZ.

A comparison with the activation energy of the electrode reactions is interesting in order to evaluate the idea of lowering the internal steam reforming rate by lowering the operating temperature and thereby spread the reforming reaction over a larger part of the cell, as described in Section 3.3. Barfod et al. [134] report activation energies of the anode reaction in the order $E_A \approx 1$ eV ≈100 kJ mol^{-1}, meaning that it is similar to that of the steam reforming reaction. A decrease in operating temperature of a specific cell will therefore not have the desired effect on spreading the conversion of methane over a larger part of the cell area. However, a lowering of the SOFC operating temperature will only be industrially relevant if new cells are developed, with a higher electrochemical activity at the lower temperatures. New types of cells with improved electrodes could show a better balance between the rates of the steam reforming and the electrochemical processes if the modifications only affect the latter.

The abbreviations that are used in both Tables 5 and 6 and Figs. 4–6, denote classical Langmuir–Hinshelwood (LH), Simple Langmuir–Hinshelwood (SLH, first order with respect to methane), and Power Law (PL). Fig. 4 shows a comparison of the rates with respect to Ni content (weight), note that the reaction rate is on a logarithmic scale. LH1 is not included in the bottom plot, because the expression is not valid for this gas composition. The large difference between the values in Fig. 4 may be caused by differences in Ni particle size for the tested catalysts. The reported Ni particle sizes for SOFC anodes are in the range 0.3–3 μm [9,35,73,79,86,83], though Iwata et al. [83] report sintering up to 10 μm particles. The Ni particles in the alumina supported catalyst used as the reference have an average particle size of 6.7 nm [40]. The study by Bebelis et al. [73] further reports small (10–20 nm) particles on top of large particles. Hence, the rate expressions with respect to Ni content are very system specific and as such, they should only be used in connection with the system they have been measured on.

The reference (ref) refers to the kinetic expression reported by Wei and Iglesia [40] over Ni on alumina support and allows comparison with the kinetics for catalysts related to industrial steam reforming. In Figs. 5 and 6 the reforming rates per Ni area or per cell area are compared, as expected, the values are much closer to each other than those in Fig. 4, so a logarithmic scale is not suited for comparing these values. Instead the two first plots represent the same data, with the first plot being on a logarithmic scale to ease the comparison with Fig. 4. The optimal comparison of catalytic reactivity is with respect to active catalyst surface area. Unfortunately only three studies on Ni-YSZ report the Ni surface area and one of these, LH1, has an exceptionally high activation energy and is only valid at one of the gas compositions that are used for comparison.

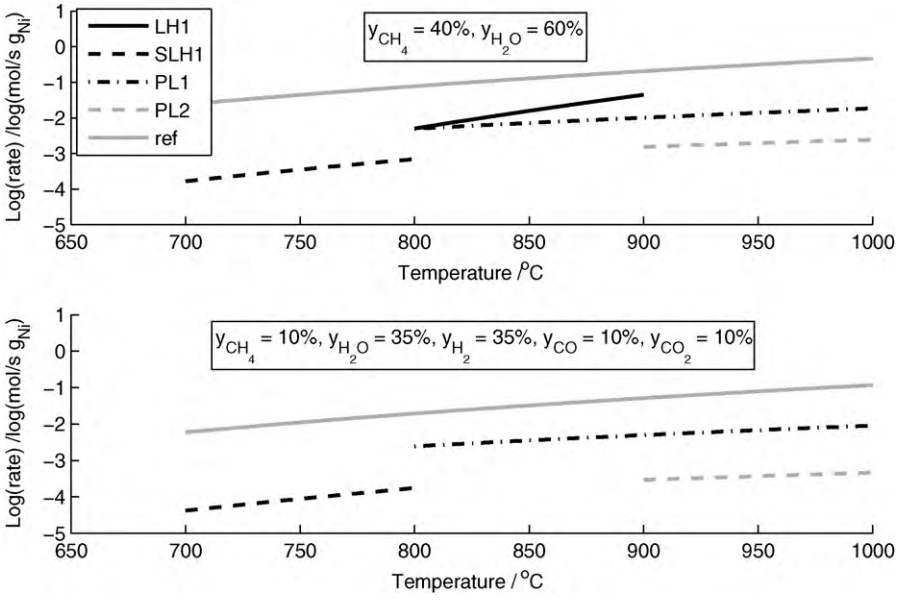

Fig. 4. Comparison of the reaction rate, at ambient pressure, of steam reforming over Ni-YSZ reported in literature with respect to nickel content: LH1 [73],SLH1 [9], PL1 [65], PL2 [125], Ref. [40].

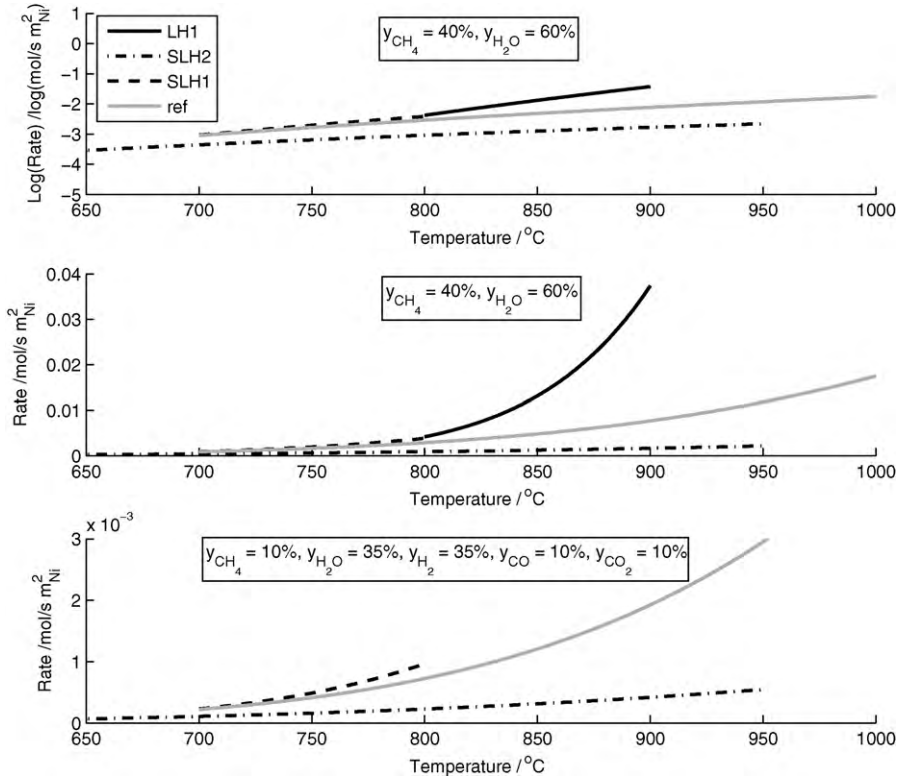

Fig. 5. Comparison of the reaction rate, at ambient pressure, of steam reforming over Ni-YSZ reported in literature with respect to nickel surface area: LH1 [73],SLH1 [9], SLH2 [79], Ref. [40].

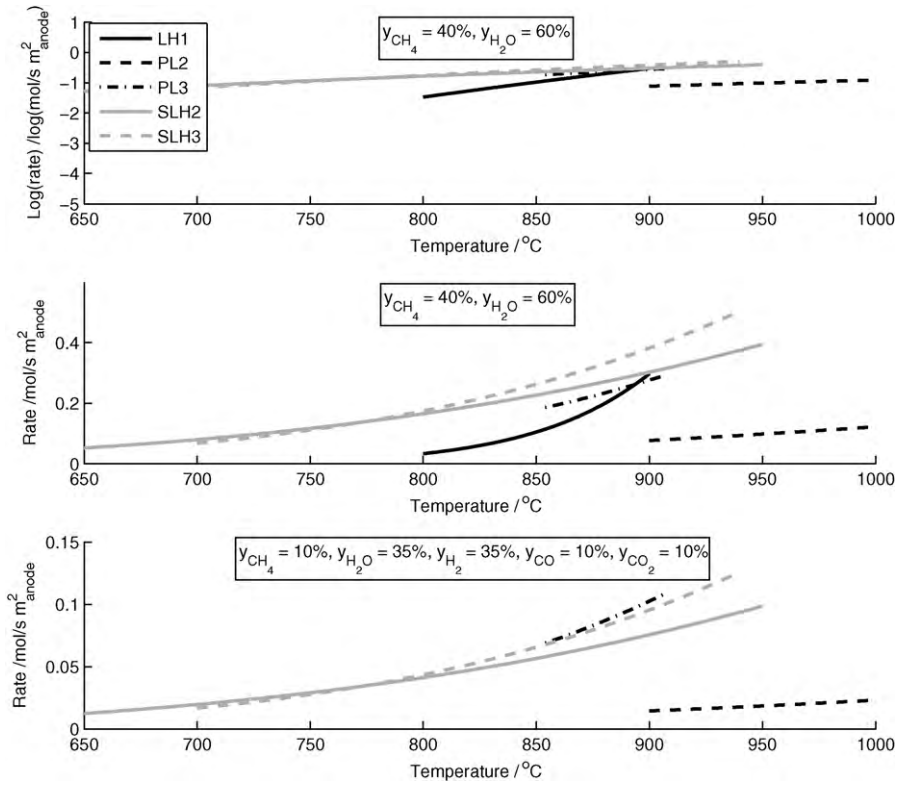

Fig. 6. Comparison of the reaction rate, at ambient pressure, of steam reforming over Ni-YSZ reported in literature with respect to geometric anode surface area: LH1 [73], PL2 [125], PL3 [124], SLH2 [79], SLH3 [109].

The reactivity predicted from these three expressions along with the reference (Ni on alumina) is shown in Fig. 5. Obviously some of the expressions that were orders of magnitudes apart in Fig. 4 are now relatively close, except for LH1 at high temperatures (note that this anode is very thick). It is especially worth noticing that the catalytic activity of the industrial catalyst is now very similar to that of the anodes, in spite of the big difference in nickel particle size, i.e. the majority of the difference when comparing based on mass is simply an effect of differences in Ni area. Only few of the kinetic studies on catalytic steam reforming over SOFC anodes explicitly report the Ni surface area, and if the Ni particle size is not given either, then an estimation of the surface is also not possible.

When comparing the measurements given as activity pr. geometric anode surface area as shown in Fig. 6, a surprisingly good correspondence is seen, especially when considering that the Ni content in these experiments range from 20 to 70 wt%. It should be noticed that all expressions in this comparison were measured over a planar cell structure, so it might not be valid for other configurations or other anode materials very different from the ones of the four studies.

The depth of the steam reforming reaction zone on Ni-YSZ anodes has been reported to be in the range 0.15–0.30 mm at 900 °C [129,133,135,136]. No systematic variation with anode thickness is found in Fig. 5, there is, however, a tendency showing that thicker anodes give higher activity. The thickest anode SLH3 (1.4 mm) gives the highest rates pr. cell area and the thinnest anode LH1 (0.01 mm) gives the second lowest rates, which indicates that the reaction depth is larger than 0.01 mm. This is supported by the fact that the thinnest anode, LH1, has the highest rate per nickel area in Fig. 5.

The rate expression that gives the lowest activity and deviates most from the others is PL2, even though the anode used to determine this expression has a thickness of 40 μm, which is a medium value for this comparison. The experiments underlying this rate were conducted with a very high conversion of methane (85–96%). This was taken into account in the data treatment by treating the anode as an integral plug flow reactor, but because of the high conversion the result are highly sensitive to small changes in the outlet composition [125]. It is not reported whether or not the cooling of the catalyst material was considered during data treatment. Note also that the activation energy reported in this study is very low, which could indicate that some mass transfer limitations are not accounted for.

In future studies, the surface area of nickel should be determined, in order to both ease comparison with other experimental studies and to increase the value of the measurements with respect to SOFC modeling work. Until further experimental studies are available, it is reasonable to use a kinetic expression from the general Ni-based steam reforming or with respect to anode surface area in a first, rough SOFC model. The relative good agreement between rates measured on different anodes, means that these expressions should result in reasonable results as also indicated from the model work performed by Nagel et al. [137] where several different kinetic expressions were used in the same model with similar results.

Hecht et al. [112] studied steam reforming kinetics over Ni-YSZ by using a setup were the porous anode was supplied with methane, water and carbon dioxide on one side and a mixture of water and carbon dioxide on the other side. No dense electrolyte was present in this setup. In this way steam reforming could be investigated under SOFC conditions, including realistic diffusion through the anode. The experimental results were compared to a dusty gas model to describe diffusion and a system of 42 elementary reactions to describe the reforming kinetics. The model results fitted the measured data well indicating the suitability of the model. A comparison of the elementary reactions and the other rate expressions in Table 5 would be interesting, both with respect to the rate and the reaction orders, but such a comparison is unfortunately not possible. Special notice should be given to the experimental setup used in this work, which is especially suited for measuring steam reforming kinetics for Ni-YSZ in an anode structure. Further experiments on this or similar setups would be valuable.

5. Water gas shift reaction

In SOFC modeling it is often assumed that the water gas shift reaction is at equilibrium at all time. Little work has been conducted to investigate this, but in several experimental works examining steam reforming kinetics, it is outlined that the water gas shift reaction was not at equilibrium [9,110,130,138,139]. Also Hecht et al. [112] include the elementary reactions of the water gas shift reaction in their model (see Section 4.4). Ahmed and Fger [138] examines the approach to the equilibrium of the reverse water gas shift reaction over a Ni/zirconia based anode. The inlet gas contains H_2 and CO_2 at different concentrations representing different levels of fuel utilization in an SOFC, but anode size and flow rates are not reported. The approach to equilibrium was defined as $100\% \cdot [1 - (P_{CO} / P_{CO,eq} - 1)]$ and is reported to be in the range 80-90% for most fuel utilizations. A few works include an expression for the water gas shift reaction rate [128,130] and the previously described set of elementary reactions by Hecht et al. [112]. If the water gas shift reaction is not at equilibrium, then the potentials of the H_2 oxidation and CO oxidation are not equal, which means that the reaction with the highest potential will drive the other reaction forward and thereby move the water gas shift reaction further toward equilibrium. The resulting cell voltage will lie between the two reaction potentials.

6. Modeling internal steam reforming

Modeling of SOFCs is being used widely, for a variety of different purposes. First of all there is the need for relative quick and cheap testing of new configurations and stack designs [10,140–145] as well as ideas for innovative system designs based on SOFCs [146–154]. These are the classical reasons for modeling. For SOFCs the further motivation comes from the fact that it is very difficult to measure the specific condition inside the cell or stack. Here modeling is an invaluable tool to evaluate concentration and temperature profiles and thereby to both avoid hotspots [155,156,126] and to determine optimal operation conditions [20,113,157–160]. An equally important use of models is as a tool in research both to interpret experimental observations [128,161,162] and to determine specific trouble areas where future research should be focused [142,161,163].

A large number of SOFC models exist that include either partial or complete internal steam reforming. A detailed rigorous model of a complete SOFC stack is highly computational demanding, so normally a SOFC model will focus on one aspect and models can roughly be divided into three categories based on the focus of the model.

Micromodels (electrode models) describe in great detail the catalytic, electrochemical and gas phase reactions in the porous electrodes, often taking into account mass and heat transfer effects as well as electrical conduction. This type of model will normally be one-dimensional and describes the performance of a cell in a single point with known bulk concentrations, this can be used to determine key issues for material research and micro structural optimization [112,163,161].

Cell/stack models examine the changes in composition and temperature in the gas channels of an SOFC and they will often have a simplified description of the electrodes and electrolyte in order to avoid excessive computations. These models are two- or three-dimensional and can be used to evaluate concentration and temperature profiles in the cell/stack, and thereby identify trou-

ble areas such as hotspots or areas with low S/C ratio. single sell models can to some extent incorporate a micro structure model [20,112,137,154,164–166].

System models describe the performance of a complete stack, they are highly simplified and are normally focused on the interaction of the stack with the surroundings. These models are zero- or one-dimensional and intended to be incorporated in flow sheets in order to evaluate and optimize complete systems which includes an SOFC [167–172,7].

When modeling an SOFC with a significant amount of methane in the inlet, the steam reforming kinetics will have a deciding influence on both the gas composition and the temperature profile both of which are major parameters in determining both the local and overall performance of the cell or stack. This means that micro structure and cell/stack models need to have an accurate description of steam reforming in order to be accurate. System models will often use a thermodynamic description, instead of kinetic expressions to describe the effect of internal reforming [171,172].

Some models describe the reforming reaction by using assumptions such as: equilibrium at all time, or 75% of the remaining CH_4 is converted in each finite element [172–178]. This approach should only be used for initial calculations for a new system or as an alternative to the thermodynamic description in system models.

The most widely used rate expression in SOFC modeling is the one found by Achenbach and Riensche [109] (SLH3 in Fig. 6) [7,20,137,154,161,163,165,166,179]. The Ni content was smaller than typical in SOFCs (20% w/w on ZrO_2), did not match the electrochemical specifications of an SOFC anode and was rather thick. From the comparison in Fig. 6 it can be seen that this expression gives a reaction rate a bit higher than average, but it is a valid choice for flow models.

Another rate expression, often used in modelling, is that found by Lehnert et al. [128] given in entry 10, Table 5, for example in modeling studies in Refs. [142–145,180–182]. It corresponds to the expression by Xu and Froment [39] on industrial catalyst. It assumes first order dependence both on methane and water. The latter is rarely observed experimentally, especially at conditions relevant for steam reforming in SOFCs (see Section 4).

In recent literature, several micro structural model works have used a complete set of elementary reactions (42 reactions), with separate kinetic expressions, to describe the catalyzed steam reforming and water gas shift reactions [112,141,159,164,183]. The accuracy of this type of models will primarily depend on how well the gas diffusion and micro structure of the anode are described. This method requires high computer power and since the kinetic data sets are taken from different studies, a comparison with the experimental data would be highly rewarding.

6.1. Recommendations

Until a consensus on the steam reforming kinetics is reached, the best choice for a steam reforming rate expression for use in a model is the use of a kinetic expression measured on the specific cell under the reaction conditions that are relevant for the model, as done by several research groups [112,126,135,162]. If this is not possible, we recommend an expression with a reaction order of methane close to 1, and E_A around 100 kJ mol^{-1}, possibly a bit lower. The dependency of water is disputed, but it seems that if there is a dependency it is slightly negative.

In micro structure models it is necessary to use a steam reforming rate with respect to Ni surface area. Only few experimental works report this for Ni-YSZ. There seems to be a close correlation to industrial steam reforming for these kinetics and the thoroughly examined expression reported by Wei and Iglesia [40] appears to be a valid choice for this type of model, even though the study was not performed on Ni-YSZ.

7. Conclusion

Optimal operation of SOFCs with internal steam reforming requires that the steam reforming reaction and the electrochemical reactions progress at similar rates. Order of magnitude calculations show that at the temperatures targeted in SOFCs today ($\approx$700 °C), the difference between the rates are now so small that it should be possible to lower the reforming rate to the same level as the electrochemical. Much work is being done on finetuning the SOFC anode material in order to achieve this, and an elegant solution would be to use the sulfur that is already present in the natural gas, to reduce the internal reforming rate by blocking the active nickel step sites. Unfortunately, sulfur increases the long-term degradation of the cell voltage and therefore it may be more viable to block the step sites with alkali metals. A completely different approach that also seems promising is to replace some of the nickel with copper. This seems to lower the catalytic activity, without having a significant influence on cell performance and, furthermore, it increases the resistance toward carbon poisoning. When considering this type of work, it is important to keep in mind that the operating temperature of SOFCs is generally being lowered, so the finetuning of the catalyst must be done with consideration to the intended operating temperature.

Another approach for optimizing internal steam reforming utilization is to carefully control the operating conditions so that existing stacks can withstand the temperature gradients that arise. This requires precise modeling, and therefore an overview of steam reforming kinetics on SOFCs was given and discussed. There are large differences in the reported steam reforming kinetics, which is reflected by the number of kinetic expressions that exist for both industrial steam reforming catalysts and on Ni-YSZ for SOFCs. Recent improved understanding of the elementary steps by surface science studies, in situ electron microscopy and DFT calculations have given the possibility to give an atomic level view and to develop micro structure models. These verify a strong positive dependence on the partial pressure of methane and a negative influence of water under conditions that are relevant for internal steam reforming in SOFCs.

SOFC models incorporating internal steam reforming have only recently been developed. Even though their number is rapidly increasing they only use a few experimental data sets. Five studies were compared with respect to the geometric surface area of the anode (Fig. 6). It is worth noticing that these anodes showed similar overall reaction rates, in spite of relatively large structural differences. Only three studies on Ni-YSZ could be compared with respect to the surface area of nickel (Fig. 5). The comparison showed a relatively good agreement, but nothing conclusive.

There is a surprising lack of detailed investigations of the catalytic activity of Ni-YSZ with respect to steam reforming, where the nickel surface area and particle size are reported and the common practice for measuring catalytic activity is followed. Such thorough experimental studies are needed to increase the precision of SOFC models with internal steam reforming.

References

[1] A.D. Rao, G.S. Samuelsen, J. Eng. Gas Turbines Power 125 (2003) 59–66.
[2] H. Itoh, M. Mori, N. Mori, T. Abe, J. Power Sources 49 (1994) 315–332.
[3] E.M. Leal, J. Brouwer, J. Fuel Cell Sci. Technol. 3 (2006) 137–143.
[4] I. EG&G Technical Services, Fuel Cell Handbook, seventh ed., U.S. Dep. Energy Office of Fossil Energy Nat. Energy Technol. Lab., 2004.
[5] J.V. Herle, Y. Membrez, O. Bucheli, J. Power Sources 127 (2004) 300–312.
[6] C. Athanasiou, F. Coutelieris, E. Vakouftsi, V. Skoulou, E. Antonakou, G. Marnellos, A. Zabaniotou, Int. J. Hydrogen Energy 32 (2007) 337–342.
[7] M. Sucipta, S. Kimijima, K. Suzuki, J. Power Sources 174 (2007) 124–135.
[8] N.F.P. Ribeiro, M.M.V.M. Souza, O.R.M. Neto, S.M.R. Vasconcelos, M. Schmal, Appl. Catal. A 353 (2009) 305–309.
[9] D.L. King, J.J. Strohm, X. Wang, H.-S. Roh, C. Wang, Y.-H. Chin, Y. Wang, Y. Lin, R. Rozmiarek, P. Singh, J. Catal. 258 (2008) 356–365.

[10] H. Yong, D. Goodwin, J. Electrochem. Soc. 155 (2008) 666–674.
[11] E. Nikolla, J.W. Schwank, S. Linic, Catal. Today 136 (2008) 243–248.
[12] J.-M. Klein, M. Henault, P. Gelin, Y. Bultel, S. Georges, Electrochem. Solid-State Lett. 11 (2008) 144.
[13] I. Gavrielatos, V. Drakopoulos, S.G. Neophytides, J. Catal. 259 (2008) 75–84.
[14] J. Rostrup-Nielsen, J. Hansen, S. Helveg, N. Christiansen, A.-K. Jannasch, Appl. Phys. A 85 (2006) 427–430.
[15] S. Georges, G. Parrour, M. Henault, J. Fouletier, Solid State Ionics 177 (2006) 2109–2112.
[16] S. Douvartzides, F. Coutelieris, A. Demin, P. Tsiakaras, AIChE J. 49 (2003) 248–257.
[17] J. Meusinger, Fuel Energy Abstr. 38 (1997) 408.
[18] R. Peters, E. Riensche, P. Cremer, J. Power Sources 86 (2000) 432–441.
[19] S. Douvartzides, P. Tsiakaras, Thermodyn. Energy Sources 24 (2002) 365–373.
[20] P. Hendriksen, Proceedings of the Fifth International Symposium on Solid Oxide Fuel Cells (SOFC-V), 1997, pp. 1319–1328.
[21] J.R. Rostrup-Nielsen, Catal. Sci. Technol. 5 (1984) 1–117.
[22] E. Ivers-Tiffe, A. Weber, D. Herbstritt, J. Eur. Ceram. Soc. 21 (2001) 1805–1811.
[23] F. Tietz, Q. Fu, V. Haanappel, A. Mai, N. Menzler, S. Uhlenbruck, Int. J. Appl. Ceram. Technol. 4 (2007) 436–445.
[24] C. Sun, U. Stimming, J. Power Sources 171 (2007) 247–260.
[25] F. Tietz, H.-P. Buchkremer, D. Stver, J. Electroceram. 17 (2006) 701–707.
[26] W. Zhu, S. Deevi, Mater. Sci. Eng. A 362 (2003) 228–239.
[27] S.P. Jiang, S.H. Chan, J. Mater. Sci. 39 (2004) 4405–4439.
[28] P. Vernoux, M. Guillodo, J. Fouletier, A. Hammou, Solid State Ionics 135 (2000) 425–431.
[29] I.V. Yentekakis, J. Power Sources 160 (2006) 422–425.
[30] M. Kawano, T. Matsui, R. Kikuchi, H. Yoshida, T. Inagaki, K. Eguchi, J. Power Sources 182 (2008) 496–502.
[31] R. Kikuchi, N. Koashi, T. Matsui, K. Eguchi, T. Norby, J. Alloys Compd. (2006) 622–627.
[32] B.C. Steele, A. Heinzel, Nature 414 (2001) 345–352.
[33] F. Baumann, J. Fleig, G. Cristiani, B. Stuhlhofer, H. Habermeier, J. Maier, J. Electrochem. Soc. 154 (2007) 931–941.
[34] P. Gannon, S. Sofie, M. Deibert, R. Smith, V. Gorokhovsky, J. Appl. Electrochem. 39 (2009) 497–502.
[35] M. Brown, S. Primdahl, M. Mogensen, J. Electrochem. Soc. 147 (2000) 475–485.
[36] J. Van herle, R. Ihringer, R. Vasquez Cavieres, L. Constantin, O. Bucheli, J. Eur. Ceram. Soc. 21 (2001) 1855–1859.
[37] N. Bodrov, L. Apel'Baum, M. Temkin, Kinet. Catal. 5 (1964) 614–622.
[38] J. Sehested, Catal. Today 111 (2006) 103–110.
[39] J. Xu, G.F. Froment, AIChE J. 35 (1989) 88–96.
[40] J. Wei, E. Iglesia, J. Catal. 224 (2004) 370–383.
[41] L.M. Aparicio, J. Catal. 165 (1997) 262–274.
[42] I. Chorkendorff, J. Niemantsverdriet, Concepts of Modern Catalysis and Kinetics, 2nd ed., Wiley-VCH, Germany, 2007.
[43] A. Avetisov, J. Rostrup-Nielsen, V. Kuchaev, J.-H. Bak Hansen, A. Zyskin, E. Shapatina, J. Mol. Catal. A: Chem. 315 (2010) 155–162.
[44] I. Dybkjr, Fuel Process. Technol. 42 (1995) 85–107.
[45] S.H. Lee, D.V. Applegate, S. Ahmed, S.G. Calderone, T.L. Harvey, Int. J. Hydrogen Energy 30 (2005) 829–842.
[46] D.-J. Liu, T.D. Kaun, H.-K. Liao, S. Ahmed, Int. J. Hydrogen Energy 29 (2004) 1035–1046.
[47] J.R. Rostrup-Nielsen, J. Catal. 11 (1968) 220–227.
[48] T. Iida, M. Kawano, T. Matsui, R. Kikuchi, K. Eguchi, J. Electrochem. Soc. 154 (2007) B234–B241.
[49] R. Cunningham, C. Finnerty, R. Ormerod, Proceedings of the Fifth International Symposium on Solid Oxide Fuel Cells (SOFC-V), 1997, pp. 973–982.
[50] S.H. Clarke, A.L. Dicks, K. Pointon, T.A. Smith, A. Swann, Catal. Today 38 (1997) 411–423.
[51] K. Eguchi, H. Kojo, T. Takeguchi, R. Kikuchi, K. Sasaki, Solid State Ionics 152-153 (2002) 411–416.
[52] W. Sangtongkitcharoen, S. Assabumrungrat, V. Pavarajarn, N. Laosiripojana, P. Praserthdam, J. Power Sources 142 (2005) 75–80.
[53] K. Sasaki, Y. Teraoka, J. Electrochem. Soc. 150 (2003) 885–888.
[54] R. Kikuchi, K. Eguchi, J. Jpn. Petrol. Inst. 47 (2004) 225–238.
[55] K. Ke, A. Gunji, H. Mori, S. Tsuchida, H. Takahashi, K. Ukai, Y. Mizutani, H. Sumi, M. Yokoyama, K. Waki, Solid State Ionics 177 (2006) 541–547.
[56] Y. Hsiao, J. Selman, Proceedings of the Third International Symposium on Solid Oxide Fuel Cells, 1993, pp. 895–903.
[57] G. Janssen, J. de Jong, J. Huijsmans, Second European Solid Oxide Fuel Cell Forum. Proceedings, vol. 1, 1996, pp. 163–172.
[58] T. Takeguchi, Y. Kani, T. Yano, R. Kikuchi, K. Eguchi, K. Tsujimoto, Y. Uchida, A. Ueno, K. Omoshiki, M. Aizawa, J. Power Sources 112 (2002) 588–595.
[59] N. Laosiripojana, S. Assabumrungrat, J. Power Sources 163 (2007) 943–951.
[60] S. Helveg, C. Lpez-Cartes, J. Sehested, P.L. Hansen, B.S. Clausen, J.R. Rostrup-Nielsen, F. Abild-Pedersen, J.K. Norskov, Nature 427 (2004) 426–429.
[61] H.S. Bengaard, J.K. Norskov, J. Sehested, B.S. Clausen, L.P. Nielsen, A.M. Molenbroek, J.R. Rostrup-Nielsen, J. Catal. 209 (2002) 365–384.
[62] O. Abild-Pedersen, F. Lytken, J. Engbk, G. Nielsen, I. Chorkendorff, J.K. Norskov, Surf. Sci. 590 (2005) 127–137.
[63] J. Rostrup-Nielsen, L. Christiansen, Appl. Catal. A 126 (1995) 381–390.
[64] J.N. Kuhn, N. Lakshminarayanan, U.S. Ozkan, J. Mol. Catal. A 282 (2008) 9–21.
[65] A. Lee, R. Zabransky, W. Huber, Eng. Chem. Res. 29 (1990) 766–773.
[66] E. Nikolla, J. Schwank, S. Linic, J. Catal. 250 (2007) 85–93.
[67] C.M. Finnerty, R.H. Cunningham, R.M. Ormerod, Radiat. Eff. Def. Solids 151 (1999) 77–81.
[68] H. Oudghiri-Hassani, S. Rakass, N. Abatzoglou, P. Rowntree, J. Power Sources 171 (2007) 850–855.
[69] N.J. Coe, R.H. Cunningham, R.M. Ormerod, Catal. Lett. 49 (1997) 189–192.
[70] Y. Lin, Z. Zhan, J. Liu, S.A. Barnett, Solid State Ionics 176 (2005) 1827–1835.
[71] Y. Lin, Z. Zhan, S.A. Barnett, J. Power Sources 158 (2006) 1313–1316.
[72] H. Zhu, A.M. Colclasure, R.J. Kee, Y. Lin, S.A. Barnett, J. Power Sources 161 (2006) 413–419.
[73] S. Bebelis, A. Zeritis, C. Tiropani, S.G. Neophytides, Eng. Chem. Res. 39 (2000) 4920–4927.
[74] B. Steele, I. Kelly, H. Middleton, R. Rudkin, Solid State Ionics 28-30 (1988) 1547–1552.
[75] E. Perry Murray, T. Tsai, S. Barnett, Nature 400 (1999) 649–651.
[76] E. Putna, J. Stubenrauch, J. Vohs, R. Gerte, Langmuir 11 (1995) 4832–4837.
[77] Park, Vohs, Gorte, Nature 404 (2000) 265–267.
[78] M. Mogensen, K. Kammer, Ann. Rev. Mater. Res. 33 (2003) 321–331.
[79] M. Boder, R. Dittmeyer, J. Power Sources 155 (2006) 13–22.
[80] D.J.L. Brett, A. Atkinson, N.P. Brandon, S.J. Skinner, Chem. Soc. Rev. 37 (2008) 1568–1578.
[81] B. Zhu, Ionics 4 (1998) 435–443.
[82] J. Akikusa, K. Adachi, K. Hoshino, T. Ishihara, Y. Takita, J. Electrochem. Soc. 148 (2001) A1275–A1278.
[83] T. Iwata, J. Electrochem. Soc. 143 (1996) 1521–1525.
[84] T. Kawada, N. Sakai, H. Yokokawa, M. Dokiya, M. Mori, T. Iwata, J. Electrochem. Soc. 137 (1990) 3042–3047.
[85] H. Itoh, T. Yamamoto, M. Mori, I. Horifa, N. Sakai, H. Yokokawa, M. Dokiya, J. Electrochem. Soc. 144 (1997) 641–646.
[86] D. Simwonis, F. Tietz, D. Stver, Solid State Ionics 132 (2000) 241–251.
[87] H. Yokokawa, H. Tu, B. Iwanschitz, A. Mai, J. Power Sources 182 (2008) 400–412.
[88] K. Sasaki, K. Susuki, A. Iyoshi, M. Uchimura, N. Imamura, H. Kusaba, Y. Teraoka, H. Fuchino, K. Tsujimoto, Y. Uchida, N. Jingo, J. Electrochem. Soc. 153 (2006) 2023–2029.
[89] S. Zha, Z. Cheng, M. Liu, J. Electrochem. Soc. 154 (2007) 201–206.
[90] J.F. Rasmussen, A. Hagen, J. Power Sources 191 (2009) 534–541.
[91] Z. Cheng, M. Liu, Solid State Ionics 178 (2007) 925–935.
[92] J. Dong, Z. Cheng, S. Zha, M. Liu, J. Power Sources 156 (2006) 461–465.
[93] Z. Cheng, S. Zha, M. Liu, J. Power Sources 172 (2007) 688–693.
[94] Y. Matsuzaki, I. Yasuda, Solid State Ionics 132 (2000) 261–269.
[95] J.B. Hansen, J. Rostrup-Nielsen, Handbook of Fuel Cells Vol. 6, John Wiley and Sons Ltd, 2009.
[96] M. Noponen, M. Halinen, J. Kiviaho, J. Saarinen, J. Fuel Cell Sci. Technol. 3 (2006) 438–444.
[97] F. Silversand, J.B. Hansen, P.J. Jannasch, A.-K, The impact of sulphur, Fuel Cell Seminar, Honululu Poster 111, 2000.
[98] J. Rasmussen, A. Hagen, The effect of H_2S on the performance of sofcs using methane containing fuel, 2010.
[99] K. Ledjeff, T. Rohrback, G. Schaumberg, Proc. 2nd Int. Symp. Solid Oxide Fuel Cells, 1991, p. 323.
[100] B. Ong, D. Mason, Fuel Cell Seminar Tuscon, 1986.
[101] P. Vernoux, J. Guindet, E. Gehain, M. Kleitz, Proceedings of the Fifth International Symposium on Solid Oxide Fuel Cells (SOFC-V), 1997, pp. 219–227.
[102] R. Gorte, P. Seungdoo, J. Vohs, W. Conghua, Adv. Mater. 12 (2000) 1465–1469.
[103] O. Costa-Nunes, R.J. Gorte, J.M. Vohs, J. Power Sources 141 (2005) 241–249.
[104] V.V. Krishnan, S. McIntosh, R.J. Gorte, J.M. Vohs, Solid State Ionics 166 (2004) 191–197.
[105] S. Li, S. Wang, H. Nie, T.L. Wen, J. Solid State Electrochem. 11 (2007) 59–64.
[106] U. Flesch, J. Meusinger, A. Naoumidis, D. Stover, Mater. Sci. Forum 308-311 (1999) 788–793.
[107] H. Zhu, R.J. Kee, M.R. Pillai, S.A. Barnett, J. Power Sources 183 (2008) 143–150.
[108] P. Aguiar, N. Lapena-Rey, D. Chadwick, L. Kershenbaum, Chem. Eng. Sci. 56 (2001) 651–658.
[109] E. Achenbach, E. Riensche, J. Power Sources 52 (1994) 283–288.
[110] R. Peters, R. Dahl, U. Klttgen, C. Palm, D. Stolten, J. Power Sources 106 (2002) 238–244.
[111] N. Nakagawa, H. Sagara, K. Kato, J. Power Sources 92 (2001) 88–94.
[112] E.S. Hecht, G.K. Gupta, H. Zhu, A.M. Dean, R.J. Kee, L. Maier, O. Deutschmann, Appl. Catal. A 295 (2005) 40–51.
[113] A. Dicks, K. Pointon, A. Siddle, J. Power Sources 86 (2000) 523–530.
[114] G. Jones, J.G. Jakobsen, S.S. Shim, J. Kleis, M.P. Andersson, J. Rossmeisl, F. Abild-Pedersen, T. Bligaard, S. Helveg, B. Hinnemann, J.R. Rostrup-Nielsen, I. Chorkendorff, J. Sehested, J.K. Norskov, J. Catal. 259 (2008) 147–160.
[115] D.W. Blaylock, T. Ogura, W.H. Green, G.J.O. Beran, J. Phys. Chem. C 113 (2009) 4898–4908.
[116] J. Wei, E. Iglesia, Phys. Chem. Chem. Phys. 6 (2004) 3754–3759.
[117] J. Wei, E. Iglesia, J. Phys. Chem. B 108 (2004) 7253–7262.
[118] J. Wei, E. Iglesia, Angew. Chem. 116 (2004) 3771.
[119] J. Wei, E. Iglesia, J. Catal. 225 (2004) 116–127.
[120] J. Wei, E. Iglesia, J. Phys. Chem. B 108 (2004) 40944103.
[121] P. Mnster, H. Grabke, J. Catal. 72 (1981) 279–287.
[122] V.D. Belyaev, T.I. Politova, O.A. Mar'ina, V.A. Sobyanin, Appl. Catal. A 133 (1995) 47.
[123] H. Timmermann, D. Fouquet, A. Weber, E. Ivers-Tiffee, U. Hennings, R. Reimert, Fuel Cells 6 (2006) 307–313.
[124] K. Ahmed, K. Foger, Catal. Today 63 (2000) 479–487.

[125] R. Odegard, E. Johnsen, H. Karoliussen, Proceedings of the Fourth International Symposium on Solid Oxide Fuel Cells (SOFC-IV), 1995, pp. 810–819.
[126] H. Yakabe, T. Ogiwara, M. Hishinuma, I. Yasuda, J. Power Sources 102 (2001) 144–154.
[127] A. Dicks, J. Power Sources 71 (1998) 111–122.
[128] W. Lehnert, J. Meusinger, F. Thom, J. Power Sources 87 (2000) 57–63.
[129] I. Drescher, W. Lehnert, J. Meusinger, Electrochim. Acta 43 (1998) 3059–3068.
[130] R. Leinfelder, Reaktionskinetische untersuchung zur methan-dampf-reformierung und shift-reaktion an anoden oxidkeramischer brennstoffzellen, Ph.D. Thesis, Der Technischen Fakultät der Universitt Erlangen-Nürnberg, 2004.
[131] Z. Yu, S.S.C. Chuang, Appl. Catal. A 327 (2007) 147–156.
[132] I. Yentekakis, S. Neophytides, A. Kaloyiannis, C. Vayenas, Proceedings of the Third International Symposium on Solid Oxide Fuel Cells, 1993, pp. 904–912.
[133] J. Meusinger, E. Riensche, U. Stimming, J. Power Sources 71 (1998) 315–320.
[134] R. Barfod, A. Hagen, S. Ramousse, P. Hendriksen, M. Mogensen, Fuel Cells 6 (2006) 141–145.
[135] W. Lehnert, J. Meusinger, E. Riensche, U. Stimming, Second European Solid Oxide Fuel Cell Forum. Proceedings, vol.1, 1996, pp. 143–152.
[136] J. Divisek, W. Lehnert, J. Meusinger, U. Stimming, Electrochem. Proc., 97-40, 1997, pp. 993–1002.
[137] F.P. Nagel, T.J. Schildhauer, S.M.A. Biollaz, S. Stucki, J. Power Sources 184 (2008) 129–142.
[138] K. Ahmed, K. Fger, J. Power Sources 103 (2001) 150–153.
[139] M. Poppinger, H. Landes, Ionics 7 (2001) 7–15.
[140] P. Costamagna, A. Selimovic, M. Del Borghi, G. Agnew, Chem. Eng. J. 102 (2004) 61–69.
[141] Y. Hao, D. Goodwin, J. Electrochem. Soc. 154 (2007) 207–217.
[142] B. Morel, J. Laurencin, Y. Bultel, F. Lefebvre-Joud, J. Electrochem. Soc. 152 (2005) A1382–A1389.
[143] B.A. Haberman, J.B. Young, Int. J. Heat Mass Transf. 47 (2004) 3617–3629.
[144] J.-M. Klein, Y. Bultel, S. Georges, M. Pons, Chem. Eng. Sci. 62 (2007) 1636–1649.
[145] J.M. Klein, S. Georges, Y. Bultel, J. Electrochem. Soc. 155 (2008) B333–B339.
[146] H. Ringel, J. Schule, D. Grunwald, Proceedings of the Fifth International Symposium on Solid Oxide Fuel Cells (SOFC-V), 1997, pp. 124–132.
[147] E. Riensche, J. Meusinger, U. Stimming, G. Unverzagt, J. Power Sources 73 (1998) 251–256.
[148] E. Riensche, J. Meusinger, U. Stimming, G. Unverzagt, J. Power Sources 71 (1998) 306–314.
[149] J. Palsson, A. Selimovic, L. Sjunnesson, J. Power Sources 86 (2000) 442–448.
[150] A. Selimovic, J. Palsson, J. Power Sources 106 (2002) 76–82.
[151] P. Nehter, J. Power Sources 157 (2006) 325–334.
[152] S. Chan, H. Ho, O. Ding, Fuel Cells 5 (2005) 25–33.
[153] S. Chan, O. Ding, Int. J. Hydrogen Energy 30 (2005) 167–179.
[154] K. Nikooyeh, A.A. Jeje, J.A. Hill, J. Power Sources 171 (2007) 601–609.
[155] A. Selimovic, Y. Jinliang, M. Rokni, B. Sunden, J. Palsson, T. Torisson, L. Sjunnesson, Fourth European Solid Oxide Fuel Cell Forum. Proceedings, vol.1, 2000, pp. 403–412.
[156] A. Selimovic, M. Kemm, T. Torisson, M. Assadi, J. Power Sources 145 (2005) 463–469.
[157] C. Bleise, J. Divisek, B. Steffen, U. Konig, J. Schultze, Proceedings of the Third International Symposium on Solid Oxide Fuel Cells, 1993, pp. 861–867.
[158] E. Achenbach, J. Power Sources 57 (1995) 105–109.
[159] H. Zhu, R.J. Kee, V.M. Janardhanan, O. Deutschmann, D.G. Goodwin, J. Electrochem. Soc. 152 (2005) A2427–A2440.
[160] H. Karoliussen, K. Nisancioglu, A. Solheim, R. Odegard, Proceedings of the Third International Symposium on Solid Oxide Fuel Cells, 1993, pp. 868–877.
[161] S. Sunde, P. Hendriksen, Proceedings of the Fifth International Symposium on Solid Oxide Fuel Cells (SOFC-V), 1997, pp. 1329–1338.
[162] E. Edwin, H. Karoliussen, R. Odegard, Proceedings of the Fifth International Symposium on Solid Oxide Fuel Cells (SOFC-V), 1997, pp. 833–843.
[163] S. Sunde, J. Electroceram. 5 (2000) 153–182.
[164] V.M. Janardhanan, O. Deutschmann, J. Power Sources 162 (2006) 1192–1202.
[165] A. Selimovic, Solid oxide Fuel Cell Modelling for sofc/gas Turbine Combined Cycle Simulations, Ph.D. Thesis, Lund Institute of Technology, 2000.
[166] S. Campanari, P. Iora, Fuel Cells 5 (2005) 34–51.
[167] R. Bove, P. Lunghi, N.M. Sammes, Int. J. Hydrogen Energy 30 (2005) 181–187.
[168] R. Bove, P. Lunghi, N.M. Sammes, Int. J. Hydrogen Energy 30 (2005) 189–200.
[169] J. Saarinen, M. Halinen, J. Ylijoki, M. Noponen, P. Simell, J. Kiviaho, J. Fuel Cell Sci. Technol. 4 (2007) 397–405.
[170] T.F. Petersen, N. Houbak, B. Elmegaard, Int. J. Thermodyn. 9 (2006) 161–169.
[171] A.K. Demin, V. Alderucci, I. Ielo, G.I. Fadeev, G. Maggio, N. Giordano, V. Antonucci, Int. J. Hydrogen Energy 17 (1992) 451–458.
[172] S.H. Chan, H.K. Ho, Y. Tian, Int. J. Hydrogen Energy 28 (2003) 889–900.
[173] H. Apfel, M. Rzepka, H. Tu, U. Stimming, J. Power Sources 154 (2006) 370–378.
[174] R.W. Sidwell, W.G. Coors, J. Power Sources 143 (2005) 166–172.
[175] M. Pfafferodt, P. Heidebrecht, M. Stelter, K. Sundmacher, J. Power Sources 149 (2005) 53–62.
[176] K. Ahmed, Y. Ramprakash, K. Foger, Fourth Eur. Solid Oxide Fuel Cell Forum. Proc vol.1, 2000, pp. 315–324.
[177] V. Antonucci, N. Giordano, P. Antonucci, E. Arato, P. Costamagna, G. Rocchini, A. Demin, Proc. Fourth Int. Symp. Solid Oxide Fuel Cells (SOFC-IV), 1995, pp. 820–828.
[178] P. Costamagna, E. Arato, P. Antonucci, V. Antonucci, Chem. Eng. Sci. 51 (1996) 3013–3018.
[179] E. Achenbach, J. Power Sources 49 (1994) 333–348.
[180] R.S. Gemmen, J. Trembly, J. Power Sources 161 (2006) 1084–1095.
[181] M. Ni, D.Y.C. Leung, M.K.H. Leung, J. Power Sources 183 (2008) 133–142.
[182] M. Ni, D.Y.C. Leung, M.K.H. Leung, J. Power Sources 183 (2008) 668–673.
[183] H. Zhu, R.J. Kee, J. Power Sources 169 (2007) 315–326.